D-2-2

Large Displacement Micro XY-Stage with Paired Moving Plates

Minoru Sasaki[1], Fuminori Bono[2], Kazuhiro Hane[2]

[1]Toyota Technological Institute, Dept. of Advanced Science and Technology
Hisakata 2-12-1, Tenpaku-ku, Nagoya 468-8511, Japan
Phone: +81-52-809-1840 E-mail: mnr-sasaki@toyota-ti.ac.jp
[2]Tohoku University, Dept. of Nanomechanics
Aza-Aoba 6-6-01 Aramaki, Aoba-ku, Sendai 980-8579, Japan

1. Introduction

The micro XY-stage is the basic device for scanning optical elements or samples, and applications with multiple probes for parallel imaging, lithography, and data storage. MEMS process can prepare the micro XY-stage with the batch fabrication. In general, displacements >10μm are difficult to realize. The required displacement in the multiple probe applications is ~100μm, which corresponds to the spacing between arrayed probes. IBM group has developed a electromagnetic scanner in the millipede project [1]. Considering the power consumption, the heat generation, and the package, the piezoelectric [2] or the electrostatic actuators are attractive. Kim et al. reported a stage having $5\times5mm^2$-shuttle surrounding by comb-drives [3]. Kwon et al. reported a stage consisting of eight L-shaped suspensions combining with rotational comb-drive actuators [4]. They have the cross-talk between x- and y-axis motions.

In this study, the micro XY-stage which can generate the displacements >100 μm is described.

2. Principle and Design

Figure 1 shows two stage designs showing the actuator structure which is decided by the single side patterning. The orthogonal relation between x- and y-axes is obtained with the accuracy of the mask. The comb finger is the linear-engaging type [5]. Figure 1(a) shows the design of the
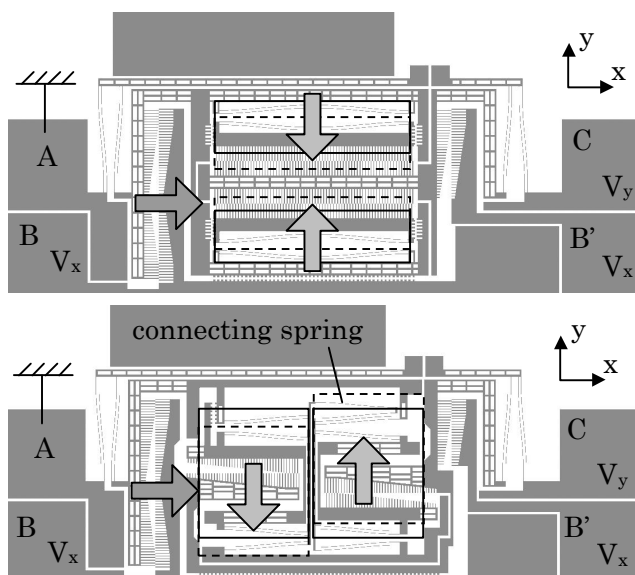
head-on counter mass for the y-axis (fast axis) movement. Two black rectangles show the plates. The fill factor (area of plate/area of total device) is 21% without including electrode pads. Two plates are connected to the actuator elements via buried oxide. With the spring connecting plates, the symmetric moving mode is generated. This cancels inertia forces working on two plates even under the fast scanning. Two moving plates work as the counter balance each other. The spring connecting moving plates is in the plate layer, and the suspension for the actuator is in the other actuator layer. This center elements are connected to the frame (see Figs. 2(a) and 2(b)), which can be driven along x-axis. Figure 1(b) shows the design of the side-on counter mass. The fill factor is 30%. The spring connecting moving plates is in the actuator layer. Electrode A is connected to
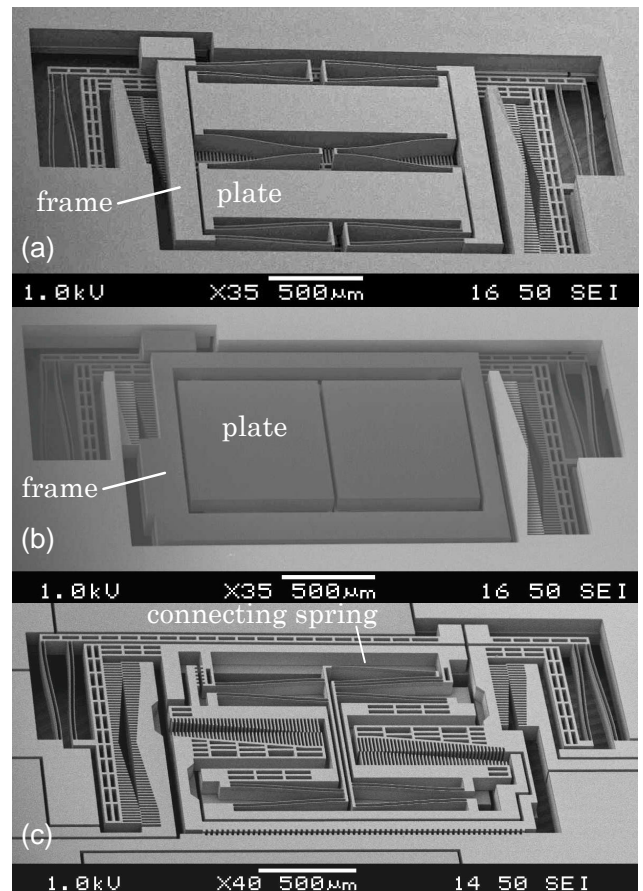

Fig. 2. Images of fabricated stage. (a) Plate side of head-on counter mass design. (b) Plate and (c) actuator sides of side-on counter mass design.

Fig. 1. (a) Head-on and (b) side-on counter mass designs of the micro XY-stage.

the ground. Electrodes B and B' are for driving along x-axis. Electrode C is for driving along y-axis. The driving voltage Vy is connected to two fixed combs for the center y-axis actuators. Two comb-drive actuators drive along mutually opposite y-axis directions.

3. Fabrication

The fabrication is anisotropic plasma Si etchings of the SOI wafer from both sides. The thicknesses of device, buried oxide, and handling layers are 100, 2, and 100µm, respectively. Vapor HF is used for the sacrificial oxide etching. Figures 2(a) and 2(b) show views from the moving plates of head-on and side-on counter mass designs, respectively. Figure 2(c) is the view from the actuators of Fig. 2(b). Structures having small holes are suspended after the sacrificial etching. The designed length of the under-etching of the buried oxide is 11µm. The buried oxide remains at thicker regions.

4. Results and Discussion

Figure 3 shows images of the stage of the side-on counter mass design. For making the inside structure clearer, the device without plates is prepared. Figure 3(a) is the initial state. Figure 3(b) is the condition driving along x- and y-axis directions at the same time.

Figure 4(a) is the static displacement obtained from the design of the head-on counter mass. The displacements along x- and y-axes are shown as a function of the square of the driving voltage V. As a feature of the linear-engaging comb actuator, the displacement curve is concave up. The displacement of 110µm (geometrical limit) is obtained at the driving voltage of 68V. For y-axis, the maximum displacement is 20µm at the driving voltage of 47V. Even under the resonant driving at 551Hz, the displacement is 40µm. This can be attributed to the spring prepared in the different layer from the actuator layer. The balance of the force generates the rotating momentum of the plate as shown in Fig. 5. This rotation disturbs the large displacement.

Figure 4(b) is from the design of the side-on counter mass. The x-axis displacement of 110µm (geometrical limit) is obtained at 70V. This is same with that of Fig. 4(a). For y-axis, the static displacement of 90µm is obtained at 125V. At the resonance (690Hz), the displacement of 115µm (geometrical limit) is obtained. The resonant frequencies are relatively higher compared to the previous researches [1]. Although the side-on counter mass remains the in-plane rotational momentum, the balancing is effective for realizing the simultaneous x- and y-axes driving.

This research is based on the previous project of the grant-in-aid for scientific research on priority areas (B) (2) (no. 12131202). The facilities used for this research include the Micro/Nano-Machining Research and Education Center at Tohoku University.
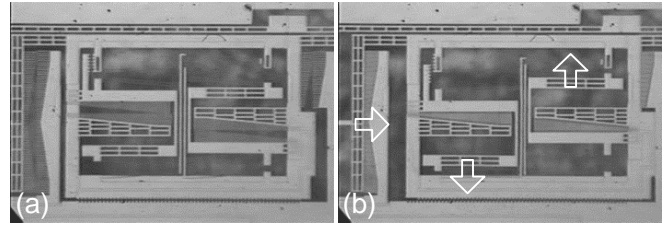

Fig. 3. Actuator at (a) initial condition and (b) driving condition along x- and y-directions.
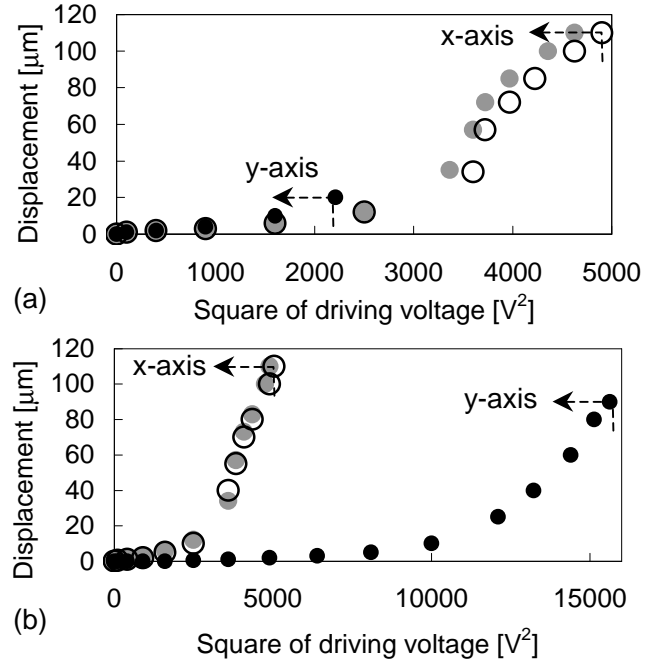

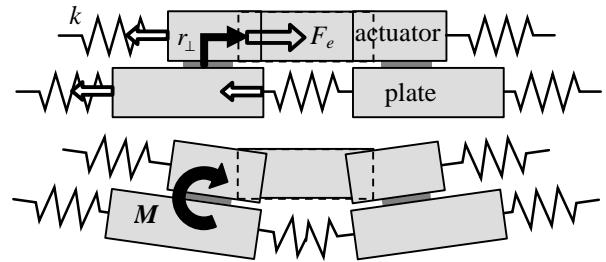Fig. 4. Static x- and y-axis displacements of (a) head-on and (b) side-on counter mass designs.

Fig. 5. Schematic drawing for explaining the generation of the out-of-plane rotation in the head-on counter mass stage design.

References

[1] H. Rothuizen, M. Despont, U. Drechsler, G. Genolct, W. Haberle, M. Lutwyche, R. Stutz, P. Vettiger, Proceedings of MEMS 2002 (2002) 582.

[2] D. Y. Zhang T. Ono, M. Esashi, Sensors & Actuators A122 (2005) 301.

[3] C. H. Kim, H.-M. Jeong, J.-U. Jeon, Y.-K. Kim, J. MEMS, 12 (2003) 470.

[4] H. N. Kwon, J.-H. Lee, K. Takahashi, H. Toshiyoshi, Digest of Transducers'05, 1C3.5 (2005) 69.

[5] J. D. Grade, H. Jerman, T. W. Kenny, J. MEMS 12 (2003) 335.